Electrooxidation of iodine on smooth platinum in aqueous media

ARTICLE *in* ANALYTICAL CHEMISTRY · MARCH 1972

Impact Factor: 5.64 · DOI: 10.1021/ac60311a009

3 AUTHORS, INCLUDING:

Rolando Guidelli
University of Florence
226 PUBLICATIONS **3,877** CITATIONS

Electro-Oxidation of Iodine on Smooth Platinum in Aqueous Media

Giorgio Raspi and Francesco Pergola
Istituto di Chimica Analitica ed Elettrochimica of University of Pisa

Rolando Guidelli
Istituto di Chimica Analitica of University of Firenze, Firenze, Italy

For pH values ranging from 1.8 to 7, the voltammogram of I^- in the absence of bromides and chlorides, as recorded toward more positive potentials, shows three successive steps, due to the electrode processes $I^- \rightarrow I_2$, $I_2 \rightarrow IOH$, and $IOH \rightarrow IO_3^-$, respectively. The appearance of a current peak between the last two steps is explained by the formation of a surface film of platinum oxides, which hinders the electro-oxidation to IO_3^-. In the presence of bromides or chlorides, the voltammogram of I^- recorded toward more positive potentials shows three steps, due to the electrode processes $I^- \rightarrow I_2$, $I_2 \rightarrow IX$ (X = Cl, Br), and $IX \rightarrow I^V$, respectively. The mean limiting current of the $IX \rightarrow I^V$ step tends to decrease rapidly with time, owing to the partial coverage of the electrode by oxidation products. The use of a pulse-polarographic technique applicable to solid electrodes has permitted the elimination of this inconvenience.

THE OXIDATION of iodide at a platinum electrode in aqueous media has been the subject of several works. Thus Kolthoff and Jordan (*1*) obtained two successive anodic waves from solutions of I^- at different pH by using a rotating platinum electrode. The first wave is well defined and corresponds to the oxidation of I^- to I_2, whereas the second is poorly defined and shows a pronounced maximum. Since the latter wave has a height equal to that of the former, the above authors ascribe it to the oxidation from I_2 to I^I. This conclusion was successively criticized by Anson and Lingane (*2*), who observed that the chronopotentiogram of iodide on platinum shows two steps. The first step was ascribed by these authors to the oxidation of I^- to I_2, whereas the second was attributed to the successive oxidation to IO_3^-. Wakkad and coworkers (*3*) obtained two anodic waves of I^- on a foil platinum electrode. The first wave was ascribed, as usual, to the oxidation of I^- to I_2, whereas the second, which exhibits a characteristic fall in current, was interpreted as an oxidation wave to HIO_2. On the contrary, Zakharov and Songina (*4*) attribute the second anodic wave, obtained by polarographing a solution of iodide on a rotating platinum electrode, to the oxidation to iodate. The height of the wave, whose limiting current decreases at sufficiently positive potentials originating a current minimum, depends on the sweep-rate of the applied potential and on the state of the electrode surface. No second wave is observed if the voltammogram is recorded from positive toward negative potentials. Beran and Bruckenstein (*5*) also state that the second anodic wave of iodide on rotated platinum disk and ring-disk electrodes in 1*M* $HClO_4$ is due to the oxidation to iodate.

The present paper deals with a voltammetric investigation of the electro-oxidation of iodide ion to species with oxidation numbers higher than 0 at a platinum microelectrode with periodical renewal of the diffusion layer (DLPRE) described by Cozzi and coworkers (*6*). This investigation has been carried out both in the presence of chlorides or bromides and in their absence. In two preceding papers Guidelli and Piccardi studied the oxidation of I_2 on platinum in acetic acid (*7*) and acetic anhydride (*8*) by using the same polarographic techniques employed in this work. For the voltammetric behavior of the systems Cl_2/Cl^-, Br_2/Br^-, and I_2/I^- in aqueous media, the reader is referred to references (*9–11*).

EXPERIMENTAL

For the recording of voltammetric and pulse-polarographic curves, the same equipment as in Reference *7* was used. The reference and counter-electrodes were saturated mercurous sulfate electrodes, joined to the cell by a bridge consisting of a solid mixture of SiO_2 and Na_2SO_4 in the ratio 3:2. All potentials reported in the present work are referred to the SCE. Buffer solutions consisting of mixtures of H_3PO_4–NaH_2PO_4, acetic acid and sodium acetate, and NaH_2PO_4–Na_2HPO_4 were used as supporting electrolytes within the pH range 1.8–3.5, 3.5–6.0, and 6.0–7.0, respectively. The ionic strength of the solutions was kept equal to 1 by adding $NaNO_3$, whenever necessary. The pH values were measured with a Metrohm E 388 potentiometer, except for the 1*M* and 0.1*M* $HClO_4$ solutions. In these cases, the pH was taken as 0 and 1, respectively.

RESULTS AND DISCUSSION

Oxidation Waves of I^- in the Absence of Bromides and Chlorides. THE OXIDATION STEP FROM I_2 TO IO_3^-. Figure 1 shows the voltammograms obtained from iodide solutions of differing concentrations in 1*M* $HClO_4$, on applying potentials increasing from +0.35 to +1.75 V to the platinum microelectrode. Curve 1, given by perchloric acid alone, exhibits an anodic peak at about +1.15 V, due to the formation of a surface layer of platinum oxides. In the presence of iodide the anodic peak, which is superimposed on the oxidation limiting current of I^- to I_2, is more pronounced as appears from curves 2, 3, 4, and 5. Furthermore, at more positive potentials a successive anodic wave is observed, which is ill defined because of the near discharge of the solvent.

(1) I. M. Kolthoff and J. Jordan, *J. Amer. Chem. Soc.*, **75**, 1571 (1953).
(2) F. C. Anson and J. J. Lingane, *ibid.*, **79**, 1015 (1957).
(3) S. E. S. El Wakkad, S. E. Khalafalla, and A. M. Shams El Din, *Recl. Trav. Chim. Pays-Bas*, **76**, 789 (1957).
(4) V. A. Zakharov and O. A. Songina, *Zh. Fiz. Khim.*, **36**, 1226 (1962).
(5) P. Beran and S. Bruckenstein, ANAL. CHEM., **40**, 1044 (1968).
(6) D. Cozzi, G. Raspi, and L. Nucci, *J. Electroanal. Chem.*, **12**, 36 (1966).
(7) R. Guidelli and G. Piccardi, ANAL. CHEM., **43**, 1639 (1971).
(8) G. Piccardi and R. Guidelli, *ibid.*, p 1646.
(9) G. Raspi, F. Pergola, and D. Cozzi, *J. Electroanal. Chem.*, **15**, 35 (1967).
(10) G. Piccardi and R. Guidelli, *J. Phys. Chem.*, **72**, 2782 (1968).
(11) R. Guidelli and F. Pergola, *J. Inorg. Nucl. Chem.*, **31**, 1373 (1969).

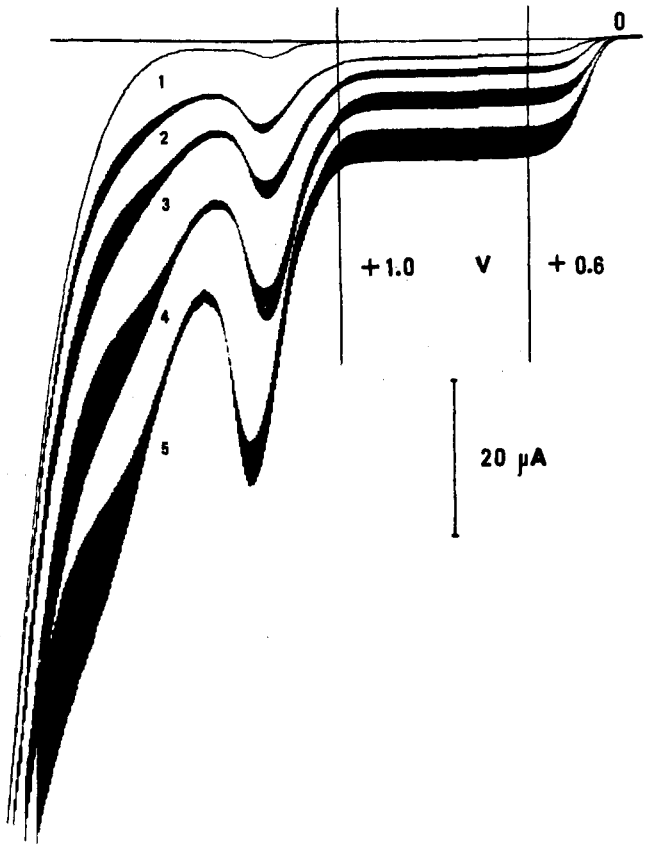

Figure 1. Voltammograms of 1M $HClO_4$ alone (curve 1) and in the presence of I^- : 1 × $10^{-4}M$ (curve 2), 2 × $10^{-4}M$ (curve 3), 4 × $10^{-4}M$ (curve 4), 7 × $10^{-4}M$ (curve 5), recorded from +0.35 V toward more positive potentials; sweep-rate 0.94 mV/sec

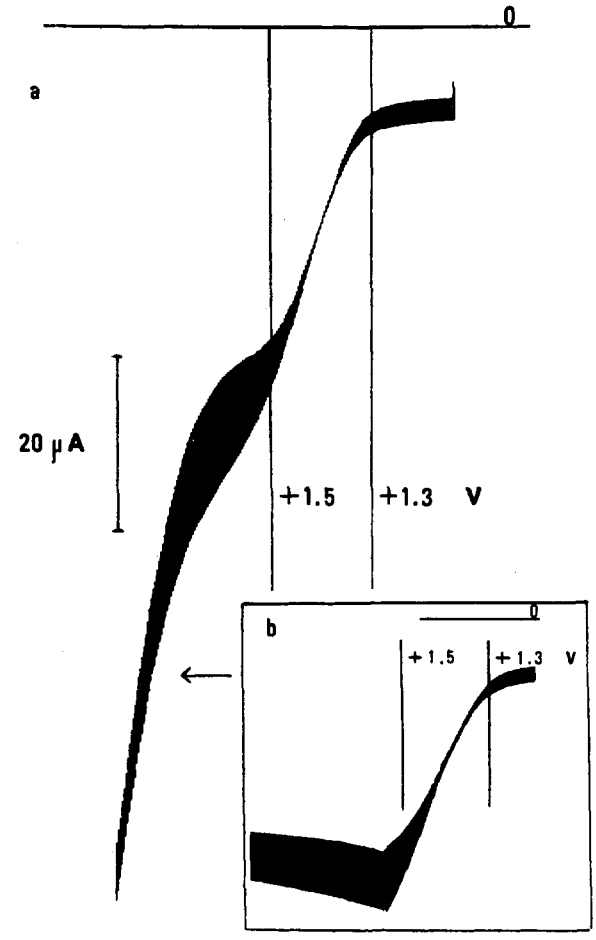

Figure 2. (*a*) Anodic step from I_2 to IO_3^- obtained by polarographing a solution of 5 × $10^{-4}M$ I^- in 1M $HClO_4$ from +1.14 V toward more positive potentials after having polarized the electrode at +1.75 V for two minutes; sweep-rate 0.94 mV/sec. (*b*) The same step in which the applied potential has been stopped at +1.55 V

The increase in the anodic peak which is observed in the presence of iodide must be attributed to the fact that on an oxide-free platinum electrode, iodide tends to be oxidized to a species with an oxidation number higher than 0 in the same potential range (~+1.00 V) within which the formation of a surface film of platinum oxides starts to take place. This film hinders the further oxidation of I_2 by increasing the overpotential relative to the corresponding electrode process. Consequently, the anodic current decreases with an increase in the applied potential, subsequently rising again at potentials sufficiently positive to permit the oxidation of I_2 at an oxide-covered platinum electrode. Starting with an oxide-free electrode, the surface layer of platinum oxides is complete at much higher potentials, the higher the rate at which the applied potential is increased. It follows that for a given concentration of iodide ion, the height of the anodic peak increases with an increase in the sweep rate. If the voltammetric curve is recorded "point by point," waiting each time for the stabilization of the current, the peak does not appear at all and the oxidation of iodide requires potentials higher than +1.30 V in order to take place. An analogous result is obtained if we previously polarize the electrode at +1.75 V and we subsequently record the voltammogram of I^-, starting from +1.14 V (at which potential the platinum oxides are already stable) and proceeding toward more positive potentials. The anodic wave so obtained (see Figure 2*a*) is five times higher than the oxidation wave of I^- to I_2, and therefore it must be attributed to the electrode process:

$$I_2 + 6H_2O \rightarrow 2IO_3^- + 12H^+ + 10e^- \qquad (1)$$

The above wave is totally irreversible and its limiting current is diffusion controlled. An anodic wave identical with the second oxidation wave of Figure 2 is obtained by polarographing a solution of I_2 under the same experimental conditions employed in this figure.

From an analysis of the anodic wave of I_2 in 1M $HClO_4$, it has been possible to draw some conclusions about the mechanism by which the oxidation of I_2 to IO_3^- proceeds. With increasing the bulk concentration, $[I_2]^*$, of I_2 the anodic wave increases proportionally to $[I_2]^*$ without shifting along the potential axis, so that the ratio $\bar{\imath}/\bar{\imath}_d$ of the mean current $\bar{\imath}$ at any given potential E to the corresponding diffusion limiting current $\bar{\imath}_d$ is constant with $[I_2]^*$. Therefore we can write:

$$\bar{\imath} = (\bar{\imath}/\bar{\imath}_d)\, K\, [I_2]^* \qquad (2)$$

where K is the proportionality constant between the diffusion limiting current and $[I_2]^*$ ($\bar{\imath}_d = K[I_2]^*$) and the ratio $\bar{\imath}/\bar{\imath}_d$ is only a function of E. On the basis of the diffusion layer approximation, the volume concentration of I_2 at the electrode surface, $[\overline{I_2}]$, can be expressed under the form:

$$[\overline{I_2}] = [I_2]^* (1 - \bar{\imath}/\bar{\imath}_d) \qquad (3)$$

From Equations 2 and 3, it immediately follows that the order ν_{I_2} of the electrode reaction 1 with respect to iodine, which is obtained from the equation

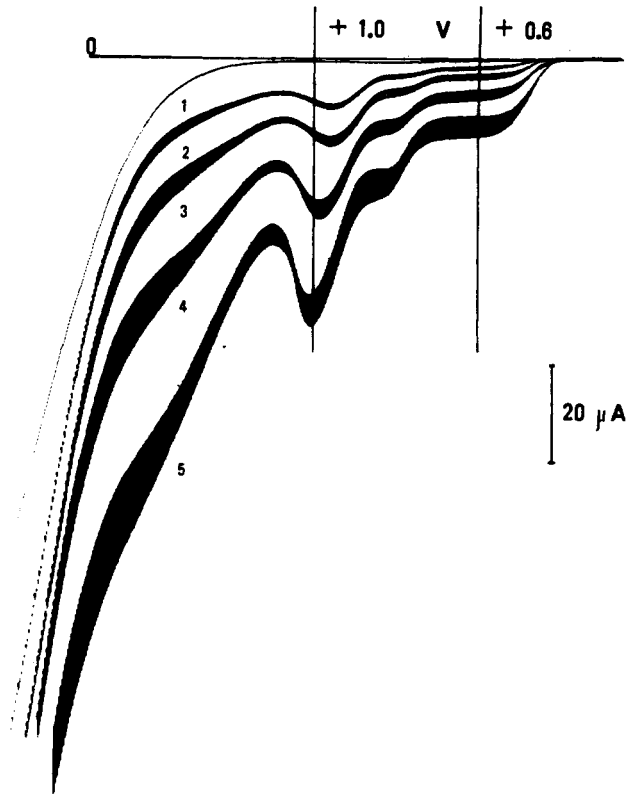

Figure 3. Voltammograms recorded from +0.25 V toward more positive potentials obtained by polarographing a pH = 4.3 buffer solution in the absence (curve 1) and in the presence of I^- : $1 \times 10^{-4}M$ (curve 2), $2 \times 10^{-4}M$ (curve 3), $4 \times 10^{-4}M$ (curve 4), $8 \times 10^{-4}M$ (curve 5). Sweep-rate 0.94 mV/sec

$$\nu_{I_2} = \left(\frac{\partial \log \bar{i}}{\partial \log [\bar{I}_2]}\right)_{E=\text{const}} \tag{4}$$

is unitary.

We are therefore allowed to use Equation 3 of reference 7 valid under the assumption that the flux of I_2 at the electrode surface is proportional to the first power of $[\bar{I}_2]$:

$$D\left(\frac{\partial[I_2]}{\partial x}\right)_{x=0} = k_b[\bar{I}_2] \tag{5}$$

where k_b is the rate constant for the oxidation process $I_2 \rightarrow IO_3^-$. By the use of the above equation, it is possible to obtain the dimensionless parameter $\lambda = k_b t_1^{1/2}/D^{1/2}$ (in which t_1 is the period of electrolysis and D the diffusion coefficient of I_2) as a function of the applied potential E. The plot of log λ against E is perfectly linear along the whole rising portion of the $I_2 \rightarrow IO_3^-$ wave and exhibits a slope of 9.4 V^{-1}. In view of the considerations made in reference 7, we can conclude that $n_0/\nu_1 + n_1\alpha = 0.51$. The above experimental data suggest that $n_0 = 0$, $n_1 = 1$, and $\alpha = 0.51$. Taking into account that the electro-oxidation of I_2 is first-order with respect to I_2 and that the rate-determining step involves the first transferring electron, this latter step can be tentatively written as follows:

$$I_2 \rightarrow I^I + I_{\text{adsorbed}} + e^- \tag{6}$$

It must be noted that the mechanism expressed by Equation 6 is surely incomplete since it does not take into account the participation of protons or hydroxyl ions either in the rate-determining step or in eventual purely chemical steps preceding the rate-determining one. Such a participation seems to be confirmed by the fact that the oxidation wave of I_2 to IO_3^- on a previously oxidized electrode, which is also observed for pH values higher than 0, shifts toward more positive potentials with increasing pH by about 40 mV per pH unit. For pH > 4, this wave is hardly distinguishable from the oxidation curve of the solvent. The retardation of the anodic process $I_2 \rightarrow IO_3^-$ produced by an increase in the hydroxyl ion concentration, which is in apparent contrast with the stoichiometry of the overall electrode Reaction 1, can be tentatively explained by the fact that, as pH increases, oxide formation proceeds more easily at the electrode surface. The increased oxide film may then cause a decrease in the heterogeneous rate of I_2 oxidation. No attempts have been made to consider the pH dependence of k_b from a quantitative point of view on these grounds, on account of the difficulties inherent in the treatment of platinum oxide formation.

If we polarize the oxidized electrode at a given potential corresponding to the plateau of the anodic wave $I_2 \rightarrow IO_3^-$, we note that the mean limiting current decreases slowly with the rest time of the electrode at this potential tending to an asymptotic value (see Figure 2*b*). The oscillographic investigation of the single potentiostatic current–time curves reveals that the more the mean limiting current decreases, the more the functional dependence of the corresponding instantaneous limiting current i upon electrolysis time t deviates from the theoretical behavior expressed by the Cottrell equation:

$$i \propto 1/t^{1/2} \tag{7}$$

Thus the product $it^{1/2}$ increases with t, instead of remaining constant. This behavior is similar to that exhibited by the current–time curves recorded at the plateau of the voltammetric curves of I_2 to I^V in acetic acid (*7*) and acetic anhydride (*8*), although much less pronounced. Here, too, the reasons for this behavior are probably to be found in the adsorption of IO_3^- at the electrode surface.

THE OXIDATION STEP FROM I^- TO IOH. The voltammograms of I^- in the absence of bromides and chlorides, as recorded between pH = 1.8 and pH = 7.0 starting from +0.25 V (at an initially oxide-free electrode) and proceeding toward more positive potentials, exhibit two anodic waves about equal in height before the appearance of the anodic peak. Figure 3 shows some voltammetric curves obtained from pH = 4.3 buffer solutions of I^- at differing concentrations of this latter ion. The first anodic wave, whose half-wave potential does not depend on pH, is the usual oxidation wave of I^- to I_2, whereas the second anodic wave is attributable to the electrode process:

$$I_2 + 2OH^- \rightarrow 2IOH + 2e^- \tag{8}$$

Since the half-wave potential of this latter wave shifts by 60 mV toward more positive values per each unitary decrement of pH, at pH 1 the wave begins to merge with the peak and consequently is no longer detectable at lower pH values.

It can be shown that the shape of the voltammogram of I^- to IOH is consistent with the assumption of a reversible overall electrode process:

$$I^- + OH^- \rightleftharpoons IOH + 2e^- \tag{9}$$

For this purpose we note that the mathematical problem relative to the diffusion of the species I^-, I_3^-, I_2, and IOH toward and from the electrode under the assumption that the electrode process of Equation 9 is reversible and that the two equilibria:

$$\frac{[IOH]\,[I^-]}{[I_2]\,[OH^-]} = K_1 \tag{10}$$

$$\frac{[I^-]\,[I_2]}{[I_3^-]} = K_2 \qquad (11)$$

are perfectly mobile is easily solved by a procedure entirely analogous to that followed in a preceding work on the aqueous system I^-–I_3^-–I_2–ICl (*10*) [see also reference (*12*) for the general treatment of homogeneous equilibria in polarography]. The theoretical current–potential characteristic is expressed by the two equations:

$$\frac{i}{i_d} = \frac{C - y}{C}\,\frac{K_1' + y + y^2/K_2}{K_1' + 2y + 3y^2/K_2} \qquad (12)$$

$$\theta_3[OH^-] \equiv \theta = \frac{(C/y - 1)K_1'}{K_1' + 2y + 3y^2/K_2} \qquad (13)$$

In these equations, i is the mean current measured at a given potential E along the rising portion of the anodic wave of I^- to IOH and i_d is the corresponding mean diffusion limiting current. Furthermore C and y are the bulk and the surface concentration of iodide, respectively, K_1' equals $K_1[OH^-]$, and θ_3 is defined by the equation:

$$\theta_3 = \exp\left[\frac{2F}{RT}(E - E_3)\right] \qquad (14)$$

where E_3 is the standard potential of the IOH/I^- couple. Figure 4 shows the experimental current–potential curve of I^- for $C = 10^{-3}M$ and pH = 5.33, together with the theoretical characteristic as obtained from Equations 12 and 13 upon giving K_2 the value 1.4×10^{-3} mole/liter determined by Katzin and Gebert (*13*) and upon attributing to K_1 the value 50 moles/liter.

The agreement between the theoretical and the experimental oxidation waves of I^- to IOH is satisfactory along the whole rising portion. The dashed curve in Figure 4 is the theoretical characteristic of I^- to IOH for the same values of C, K_1, and pH, as expressed by the equation:

$$\frac{i}{i_d} = \frac{1}{2} - \frac{(\theta - 1)\,[\theta + 1 - \sqrt{(\theta + 1)^2 + 8C\theta/K_1'}]}{8C\theta/K_1'} \qquad (15)$$

which is immediately obtained from Equations 12 and 13 upon neglecting Equilibrium 11. It is apparent that, although the less positive portion of the theoretical characteristic accounting for Equilibrium 9 is more drawn out than the corresponding portion of the theoretical characteristic neglecting I_3^- formation, both characteristics exhibit nearly the same value of $E_{3/4} - E_{1/4}$, where $E_{3/4}$ and $E_{1/4}$ designate the potential values corresponding to $i/i_d = {}^3/_4$ and ${}^1/_4$. By considerations analogous to those in Reference *10*, from Equation 15 it follows that:

$$K_1' \equiv K_1[OH^-] = \frac{\theta_{3/4}\,C}{(\theta_{3/4} - 2)^2 - 1} \qquad (16)$$

where

$$\theta_{3/4} \equiv \exp\left[\frac{F}{RT}(E_{3/4} - E_{1/4})\right] \qquad (17)$$

Since $\theta_{3/4}$ is always $\gg 1$ within the pH range investigated, Equation 16 can be simplified as follows:

$$E_{3/4} - E_{1/4} = -\frac{2.3RT}{F}\,\mathrm{pH} + \frac{2.3RT}{F}\log\frac{C}{K_1} + \frac{2.3RT}{F}\,pK_w \qquad (18)$$

(12) R. Guidelli and D. Cozzi, *J. Phys. Chem.*, **71**, 3020; 3027 (1967).
(13) L. I. Katzin and E. Gebert, *J. Amer. Chem. Soc.*, **77**, 5814 (1955).

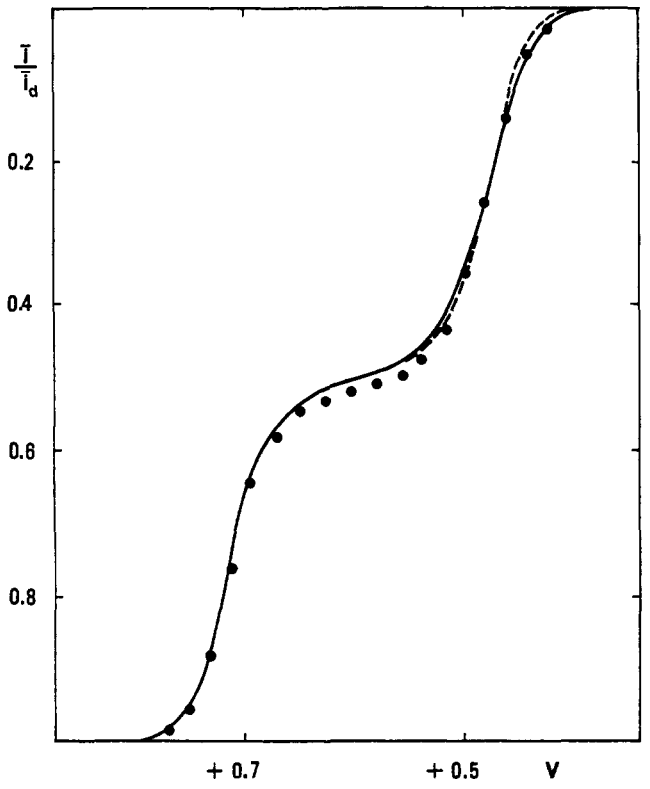

Figure 4. Overall oxidation wave of I^- to I^1

The solid curve expresses the theoretical current-potential characteristic derived from Equations 12 and 13 for pH = 5.33, $C = 1 \times 10^{-3}$ mole/liter, $K_1 = 50$ moles/liter, $K_2 = 1.4 \times 10^{-3}$ mole/liter, whereas the dashed curve expresses the characteristic derived from Equation 15 for the same values of pH, C, and K_1 upon neglecting I_3^- formation. The circles express experimental values

Equation 18 predicts that the plot of $E_{3/4} - E_{1/4}$ against pH should be linear with a slope of about −60 mV at 25 °C. The above theoretical expectations have been verified experimentally, as shown in Figure 5. Here the circles denote experimental values of $E_{3/4} - E_{1/4}$ as derived from the voltammograms of 10^{-3} and $10^{-4}M$ I^- on oxide-free platinum at differing acidities, whereas the solid straight lines express the theoretical dependence of $E_{3/4} - E_{1/4}$ upon pH as deduced from Equation 18 on setting $K_1 = 50$ moles/liter and $pK_w = 14$.

The oxidation to IOH does not take place at an oxide-covered platinum electrode. Thus, if we record the voltammogram of I^- for pH values ranging from 1.8 to 7.0 starting with an oxide-covered electrode and proceeding toward decreasing potentials, the rising portion of the oxidation step from I^- to I_2 is reached without encountering the oxidation step from I_2 to IOH. The above experimental fact can be explained by the two different hypotheses: the charge-transfer step $I_2 \rightarrow$ IOH is irreversible on oxide-covered platinum and, at the same time, the homogeneous disproportionation Equilibrium 10 yielding IOH from I_2 even in the absence of the $I_2 \rightarrow$ IOH charge-transfer step is very sluggish; both the charge-transfer steps $I^- \rightarrow I_2$ and $I_2 \rightarrow$ IOH are irreversible on oxide-covered platinum. In this latter case, the assumption of a perfectly mobile disproportionation Equilibrium 10 may still be retained.

The hypothesis of a very sluggish Equilibrium 10 contrasts with the fact that the first anodic step $I^- \rightarrow I_2$ at an oxide-free electrode is slightly higher than the successive $I_2 \rightarrow$ IOH step (see Figures 3 and 4). Thus, if Equilibrium 10 were attained very slowly around the electrode, the two diffusion-

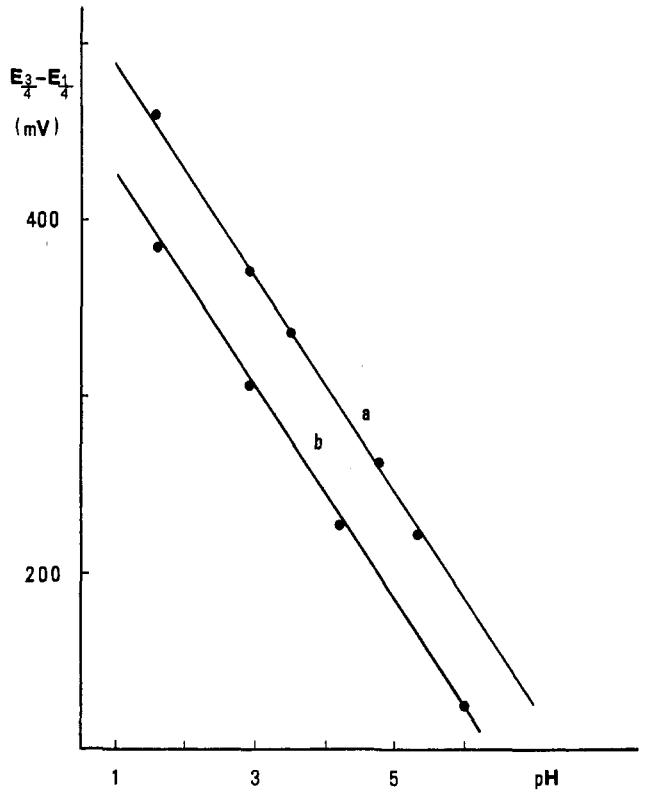

Figure 5. Values of $E_{3/4} - E_{1/4}$ against pH as obtained from the voltammograms of $1 \times 10^{-3}M$ I^- (curve *a*) and $1 \times 10^{-4}M$ I^- (curve *b*)

The straight lines express the theoretical dependence of $E_{3/4} - E_{1/4}$ upon pH for log $K_1 = 1.7$, $pK_w = 14$, and C is equal to 10^{-3} and $10^{-4}M$, respectively

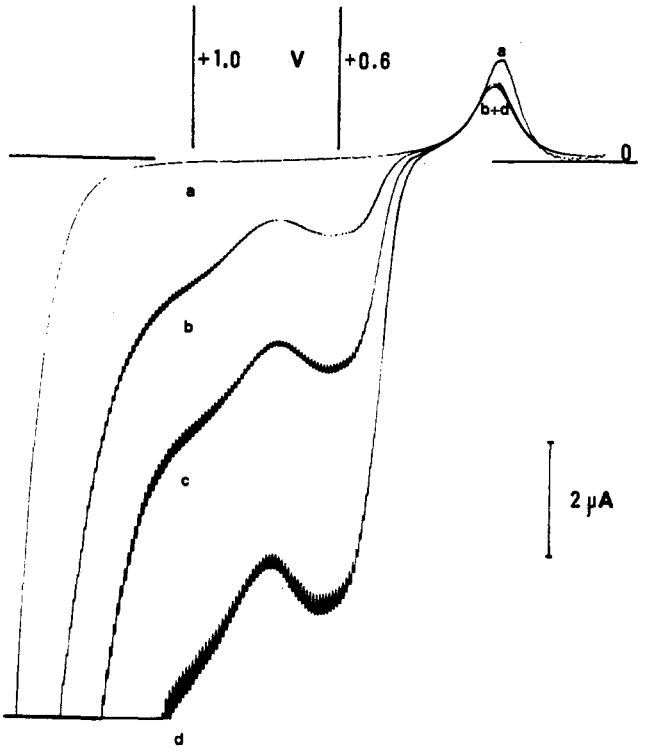

Figure 6. Voltammograms recorded from +1.5 V toward less positive potentials obtained by polarographing a pH 4 buffer solution in the absence (curve *a*) and in the presence of I^-: $1 \times 10^{-4}M$ (curve *b*), $2 \times 10^{-4}M$ (curve *c*), $4 \times 10^{-4}M$ (curve *d*); sweep-rate = 9.4 mV/sec.

controlled limiting currents of I^- to I_2 and to IOH, respectively, should be exclusively determined by the flux of I^- toward the electrode and therefore the latter should be exactly twice as high as the former. The difference in height between the two successive anodic steps from I^- to I_2 and from I_2 to IOH can only be explained by assuming the perfect mobility of Equilibrium 10 and also the existence of an appreciable difference between the diffusion coefficients of the species I^-, I_2, and IOH. A still greater difference between the heights of the $I^- \rightarrow I_2$ and the $I_2 \rightarrow I^I$ step is encountered in the presence of chlorides (*10*), in which case the ratio of the height of the $I^- \rightarrow I_2$ step to that of the $I_2 \rightarrow$ ICl step is about equal to 1.4. Here, too, we must assume that the diffusion coefficients of the various diffusing species (I^-, I_2, I_2Cl^-, ICl, ICl_2^-) are quite different and that the disproportionation equilibrium $I^- + ICl \rightleftharpoons I_2 + ICl^-$, which is analogous to Equilibrium 10, is perfectly mobile (*10*).

On the other hand the assumption of an irreversible $I^- \rightarrow I_2$ step on oxidized platinum is in apparent contrast with the fact that this step, as reached starting from an oxide-covered electrode and proceeding toward decreasing potentials, is polarographically reversible. A more thorough investigation of the voltammetric curve of I^- as registered toward decreasing potentials shows, however, that for sufficiently high sweep-rates the plateau separating the $I_2 \rightarrow IO_3^-$ step from the $I^- \rightarrow I_2$ step exhibits a depression (see Figure 6), whose area is practically independent of the bulk concentration of iodide ion. Such a depression can be attributed to the fact that part of the iodide ion diffusing toward the electrode is engaged in a purely chemical reaction with the surface layer of platinum oxides, giving rise to a sort of platinum iodide. Clearly this fraction of the iodide diffusing toward the electrode does not contribute to the flow of the current across the metal–solution interphase. The rate of the above heterogeneous chemical reaction tends to increase with an increase in the volume concentration of iodide at the electrode surface—*i.e.*, the more the rising portion of the $I^- \rightarrow I_2$ step is approached. On the other hand, the progressive depletion of platinum oxide, due to its interaction with I^- as we proceed toward less positive potentials, reduces the rate of platinum iodide formation. This may explain the round-shaped depression on the limiting current of I^- to I_2. The different nature of the surface film covering the electrode along the rising portion of the $I^- \rightarrow I_2$ step (as recorded toward less positive potentials) with respect to the platinum oxide film covering the electrode within the same potential range in the absence of I^- is further confirmed by the following observation. The cathodic peak due to the electroreduction of platinum oxides as given by a solution of supporting electrolyte in the absence of iodide ion (peak *a* in Figure 6) is slightly shifted with respect to the analogous reduction peak as obtained in the presence of I^- at the foot of the $I^- \rightarrow I_2$ step (peaks *b–d* in Figure 6). In order to exclude the possibility that the depression on the limiting current of I^- to I_2 in Figure 6 may be due to the chemical interaction of a fraction of the I^- ions diffusing toward the electrode with eventual iodate adsorbed on the electrode surface along the rising portion of the $I_2 \rightarrow IO_3^-$ wave, the following experiment was performed. After having pre-oxidized the electrode at +1.65 V in a solution of the supporting electrolyte, the potential applied to the electrode was shifted to a value of +1.0 V, corresponding to the beginning of the rising portion of the $I_2 \rightarrow IO_3^-$ step. The voltammogram recorded from +1.0 V toward less positive potentials immediately after having added I^- to the solution still exhibits a depres-

sion identical to those in Figure 6, although in the present case no iodate has had the possibility to form on the electrode surface.

In light of the previous experimental results, it is not unreasonable to assume that the $I^- \rightarrow I_2$ charge-transfer step is actually polarographically irreversible at an oxide-covered platinum electrode but reversible on the modified electrode surface (presumably covered by a layer of platinum iodide) on which the rising portion of the $I^- \rightarrow I_2$ wave in Figure 6 develops. The hypothesis according to which the charge-transfer step $I^- \rightarrow I_2$ is considered to be polarographically irreversible at a superficially oxidized platinum electrode and according to which the disproportionation Equilibrium 10 is considered to be perfectly mobile seems therefore more reliable than the alternate one in order to explain the disappearance of the $I_2 \rightarrow$ IOH step when starting with an initially oxide-covered electrode.

Oxidation Waves of I^- in the Presence of Bromides and Chlorides. The differences between the voltammetric behavior of iodide on platinum in the absence of bromides and chlorides and in their presence are not substantial. The main difference is represented by the fact that, upon recording the voltammetric curve of I^- toward more positive potentials at an initially oxide-free electrode in the presence of bromides or chlorides, the oxidation step to I^V is reached without observing any anodic peak of the type shown in Figure 1. The reason for this behavior resides in the fact that, within the potential range investigated, the surface layer of platinum oxides which is the indirect cause of the peak appearance is not stable in the presence of Br^- and Cl^-, because of the complexing action of these latter ions upon platinum oxides (*14*). Thus, the voltammogram given by I^- in 1*M* $HClO_4$ in the presence of chlorides upon applying potentials increasing from +0.25 V to +1.75 V to the electrode, shows three consecutive anodic steps, corresponding, respectively, to the oxidation of I^- to I^0 (under the form of I_2 and I_2Cl^-), to I^I (under the form of ICl and ICl_2^-), and to I^V (presumably under the form of IO_3^-). Figure 7*a* shows some voltammograms recorded under the conditions previously described for differing concentrations of I^- in the presence of 2×10^{-3} *M* Cl^-. From the figure it is evident that the oxidation wave of Cl^- to Cl_2 develops at potentials more positive than those corresponding to the electro-oxidation of I^- to I^V. In practice, if the ratio between the bulk concentrations of Cl^- and I^- is greater than 20, the oxidation wave of Cl^- to Cl_2 completely conceals the oxidation step from I^I to I^V. Likewise, the voltammogram furnished by I^- in 1*M* $HClO_4$ in the presence of bromides upon applying potentials increasing from +0.25 V to +1.65 V to the electrode, shows three consecutive anodic waves, corresponding, respectively, to the stepwise oxidation of I^- to I^0 (under the form of I_2 and I_2Br^-), to I^I (under the form of IBr and IBr_2^-), and to I^V (presumably under the form of IO_3^-). In the present case, however, the oxidation wave of Br^- to Br_2 develops at potentials less positive than those corresponding to the oxidation from I^I to I^V. Consequently, if Br^- is in excess with respect to I^-, the wave $Br^- \rightarrow Br_2$ interposes between the two anodic waves $I^0 \rightarrow I^I$ and $I^I \rightarrow I^V$ given by iodide. Thus curve 1*a* in Figure 8, obtained from a solution of 5×10^{-4}*M* I^- and 5×10^{-4}*M* Br^- in 1*M* $HClO_4$ exhibits exclusively the three anodic steps $I^- \rightarrow I^0$, $I^0 \rightarrow I^I$, and $I^I \rightarrow I^V$. In the voltammograms 2*a* and 3*a* of the same figure, obtained by doubling and quadrupling the concentration of hydrobromic acid, respectively, the oxidation wave of Br^- to Br_2 also appears. Here, too, a strong excess of Br^- with respect to I^- causes the $I^I \rightarrow I^V$ step to be poorly defined.

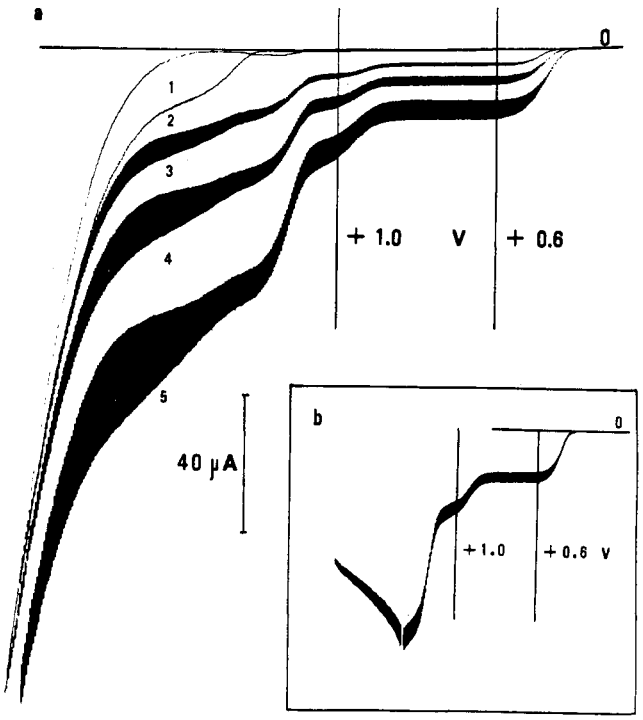

Figure 7. (*a*) **Voltammograms recorded from +0.25 V toward more positive potentials obtained by polarographing a solution of 1*M* $HClO_4$ alone (curve 1), a solution of 2×10^{-3}*M* HCl in 1*M* $HClO_4$ (curve 2) and I^- : 2.5×10^{-4}*M* (curve 3), 5×10^{-4}*M* (curve 4), 1×10^{-3}*M* (curve 5) in the presence of 2×10^{-3}*M* HCl and 1*M* $HClO_4$; sweep-rate = 0.94 mV/sec. (*b*) Curve 5 in which the applied potential has been stopped at +1.25 V**

The detailed study of the two reversible steps $I^- \rightarrow I^0$ and $I^0 \rightarrow I^I$ in the presence of an excess of bromides and chlorides, as well as of the influence exerted upon these steps by a change in the concentrations of I^-, Cl^-, and Br^- has been the subject of two previous works (*10*, *11*). Here we shall limit ourselves to the consideration of the $I^I \rightarrow I^V$ step.

If the electrode potential is held constant at a value corresponding to the limiting current of the voltammetric step $I^I \rightarrow I^V$ as recorded at an oxide-free electrode in the presence of chlorides or bromides, the mean limiting current decreases with time rather rapidly, tending toward a steady-state value (see Figures 7*b* and 8*b*). This behavior is similar to that exhibited by the oxidation wave of I_2 to IO_3^- in the absence of chlorides and bromides, although in the presence of these latter ions it is more pronounced. Thus the limiting current attained at the end of the recording of the whole voltammetric curve of I^- to I^V in the presence of chlorides is lower than the current which would be expected for an exchange of 6 electrons per iodine atom. This is clearly shown in Figure 7*a*, where the height of the $I^I \rightarrow I^V$ step recorded at a sweep-rate of 0.94 mV/sec is only twice that of the preceding $I^0 \rightarrow I^I$ step, and not four times greater, as expected. Analogously, the height of the $I^I \rightarrow I^V$ step in the presence of bromides should be five times greater than the height of the preceding $I^0 \rightarrow I^I$ step, in accordance with the overall electrode process

$$IBr \rightarrow I^V + {}^1/_2Br_2 + 5e^- \qquad (19)$$

whereas from Figure 8 it appears appreciably lower.

(14) F. C. Anson and J. J. Lingane, *J. Amer. Chem. Soc.*, **79**, 4901 (1957).

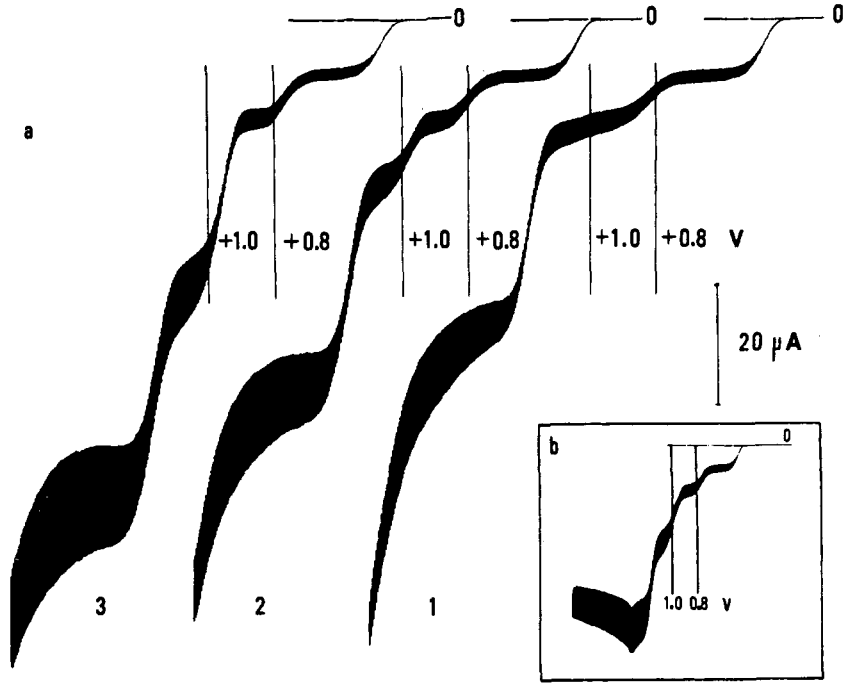

Figure 8. (*a*) Voltammograms of $5 \times 10^{-4}M$ I^- in $1M$ $HClO_4$ in the presence of HBr: $5 \times 10^{-4}M$ (curve 1), $1 \times 10^{-3}M$ (curve 2) and $2 \times 10^{-3}M$ (curve 3) recorded from +0.25 V toward more positive potentials; sweep-rate = 0.94 mV/sec. (*b*) Voltammogram of $5 \times 10^{-4}M$ I^- and $1.5 \times 10^{-3}M$ HBr in $1M$ $HClO_4$, in which the applied potential has been stopped at +1.31 V

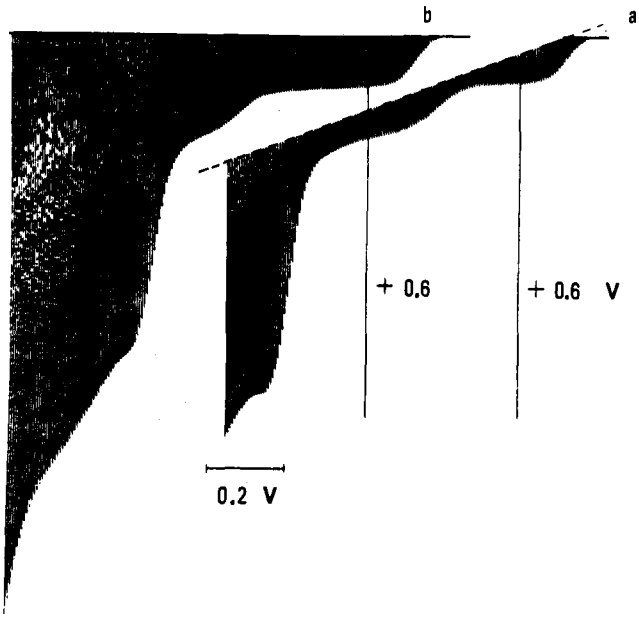

Figure 9. Pulse-polarogram of $1 \times 10^{-3}M$ I^- in $1M$ $HClO_4$, in the presence of $1 \times 10^{-3}M$ Br^- (curve *a*) and $2 \times 10^{-3}M$ Cl^- (curve *b*), respectively. Initial potential E_i = +0.30 V; t_i = 5 sec; t_f = 3 sec

It is interesting to note that if the DLPRE is immersed in a solution of I^- and Cl^- in $1M$ $HClO_4$ and the applied potential is caused to pass instantaneously from an initial value E_i = +0.3 V (at which potential no electrolysis of I^- takes place) to a final value E_f = +1.24 V, corresponding to the limiting current of the $I^I \rightarrow I^V$ step, then the current–time curve recorded at the final potential with an oscilloscope obeys the Cottrell equation, and therefore is diffusion-controlled. If we subsequently keep the applied potential at the final value E_f = +1.24 V and we submit the electrode to a series of periodic "washings" (see Reference *11*), then the potentiostatic current–time curves recorded between a washing and the successive one, while progressively decreasing with respect to the first curve recorded at E_f, tend to deviate from the Cottrell equation, approaching steady-state conditions. The plot of $(i_t/i_d)/[1-(i_t/i_d)]$ *vs.* $t^{1/2}$ (where i_t is the instantaneous current at E_f after the attainment of steady-state conditions, as measured at a given time t from the immediately preceding washing, and i_d is the corresponding instantaneous diffusion limiting current at the same electrolysis time t, as obtained from the first current–time curve recorded at E_f) is linear and passes through the origin. Relation 24 of Reference *7* is therefore obeyed. We can conclude that, in analogy with what was observed in acetic acid and acetic anhydride, the progressive lowering of the mean limiting current of the $I^I \rightarrow I^V$ step which is encountered with the conventional polarographic technique upon holding the applied potential at a constant value, must be attributed to the gradual coverage of the electrode by iodate ions (or by some other products of the electro-oxidation of I^- to the oxidation state +5). Here, too, as in acetic acid and acetic anhydride, the fall in the mean limiting current of the $I^I \rightarrow I^V$ step can be eliminated by the use of the pulse-polarographic technique described by Piccardi and Guidelli (*15*). As opposed to what was observed with the anodic pulse-polarograms of I_2 to I^V in CH_3COOH and $(CH_3CO)_2O$ (see References *7* and *8*), the inconveniences due to the adsorption of the oxidation products on the electrode surface can be eliminated by pre-treating the electrode at the potential E_i = +0.3 V for a relatively short period t_i. Furthermore the instantaneous current flowing during t_i, which is cathodic in nature, is of the same order of magnitude as the anodic current flowing during t_f at the potential E_f, at least before the washing of the electrode causes the cathodic current to drop abruptly to zero. The above experimental findings seem to indicate that at the initial potential E_i, the oxidation products adsorbed on the electrode are not simply removed mechanically from the electrode. In this connection we can assume that the adsorbed I^V is electroreduced at E_i, although it seems more probable that the iodide ions diffusing toward the electrode during t_i react chemically with the I^V both adsorbed on the electrode and distributed

(15) G. Piccardi and R. Guidelli, *Ric. Sci.*, **38**, 247 (1968).

within the diffusion layer, giving rise to I_2, which in its turn is reduced to I^-.

The pulse-polarogram of $10^{-3}M$ I^- in $1M$ $HClO_4$ and $10^{-3}M$ Cl^- as obtained upon holding the electrode at a potential E_i = +0.30 V for a period t_i of 5 sec (during which time the electrode is "washed") and, subsequently, at a potential E_f (varying from +0.30 V up to +1.51 V throughout the whole recording) for a period t_f of 3 sec, is shown in Figure 9*b*. From the figure it is evident that the first two waves are analogous to the corresponding waves in Figure 7, obtained by the conventional polarographic method, whereas the third wave is about four times higher than the first one, in accordance with the assumption of an oxidation step from I^I to I^V. Analogously, the three-step pulse-polarogram of an iodide solution in the presence of Br^- (Figure 9*a*) is such that the third step is five times higher than the first one, in accordance with the assumption of an oxidation from IBr to I^V and ½ Br_2.

The rising portion of the $I^I \rightarrow I^V$ step of the pulse-polarograms of iodide in $1M$ $HClO_4$ in the presence of bromides and chlorides has been examined in order to draw some conclusions about the mechanism of the corresponding electrode process, using the same procedure followed in connection with the $I_2 \rightarrow IO_3^-$ step of Figure 2*a*. Here, too, the plot of the logarithm of $\lambda = k_b t_f^{1/2}/D^{1/2}$ against E_f is linear. The value of $(n_0/\nu_1 + n_1\alpha)$ derived from the slope of this plot equals 0.83 in hydrobromic acid media and 0.85 in hydrochloric acid media. The above values seem to suggest that, in both cases, the charge-transfer step determining the rate of the overall electrode process $I^I \rightarrow I^V$ is the first one ($n_0 = 0$) and that such a step involves one electron ($n_1 = 1$). It has been impossible to ascertain the eventual participation of either Br^- or Cl^- in the rate-determining step owing to the impossibility of varying the bulk concentrations of these species within a sufficiently large range without causing the obliteration of the $I^I \rightarrow I^V$ step by part of the oxidation waves of Cl^- to Cl_2 or of Br^- to Br_2.

RECEIVED for review December 30, 1969. Resubmitted October 17, 1970. Accepted October 13, 1971. The present work was partially supported by C.N.R. (Consiglio Nazionale delle Ricerche) under contracts N. 115.1332.0–0469 and N. 115.1642.0–4400.

Solutions of Copper(I) Thiocyanate in Molten Tetra-*N*-Pentylammonium Thiocyanate

Michael A. Kowalski and George W. Harrington

Temple University of the Commonwealth System of Higher Education, Department of Chemistry, Philadelphia, Pa., 19122

The electrical conductivity, viscosity, infrared and visible spectra of solutions of copper(I) thiocyanate in molten tetra-*N*-pentylammonium thiocyanate were studied. Solubility was also determined. From these measurements and by comparison with similar measurements of silver and cadmium solutions, the copper species in solution was shown to be a dimer at low concentrations and a polymer at high concentrations.

IN A PREVIOUS publication from this laboratory (*1*), a study of the density, solubility, and conductometric titration curves of the binary fused salt systems silver thiocyanate/tetra-*n*-pentylammonium thiocyanate (TPNSCN) and cadmium thiocyanate/TPNSCN was reported. The results were interpreted as indicating the presence of complex species in the melts of formulas $Ag(SCN)_2^{1-}$ and $Cd(SCN)_6^{3-}$.

Although quaternary ammonium salts, like TPNSCN, are similar to alkali metal salts with respect to cationic charge, their charge densities are so much smaller that their usefulness as solvents for inorganic compounds is limited. Whereas molten alkali metal salts dissolve many inorganic compounds, these organic melts are of use as solvents only for complexable metal ions. In addition, the structures of the complexes formed in the organic melts may differ from those expected in aqueous solution because of the low cationic charge density and liquid structure. The investigation of metal ions in TPNSCN was extended to CuSCN solutions in order to determine the nature of the complex cuprous ions which would be formed in this medium.

EXPERIMENTAL

The preparation of TPNSCN, AgSCN, and $Cd(SCN)_2$ and the binary salt solutions as well as the apparatus for measurement of density and conductivity were as reported earlier (*1*, *2*).

The most concentrated solution of CuSCN in TPNSCN was prepared by mixing the solid salts in a 3:1 CuSCN to TPNSCN molar ratio and stirring with N_2 overnight at 90 °C. Equilibration for considerably longer periods did not alter the final solubility results. The resulting mixture of solid CuSCN and CuSCN-TPNSCN solution was then filtered, with the aid of a steam-jacketed funnel, to remove the undissolved metal salt. Samples of the saturated solution were analyzed for Cu content by electrodeposition from aqueous solution (*3*).

CuSCN was obtained commercially and was found, after oven drying (110 °C) and vacuum storage, to be >99% pure.

Viscosities (kinematic) were determined in an Ostwald–Cannon-Fenske type viscosimeter (size No. 300). The viscosimeter was calibrated with pure TPNSCN using published data for 60 to 100 °C (*4*).

Temperature was controlled to ±0.05 °C for density, conductivity, and viscosity determinations, by immersion of the apparatus in a thermostated oil bath.

Infrared spectra of CuSCN-TPNSCN solutions were obtained with a Beckman IR-9 Infra Red Spectrophotometer

(1) P. Keller and G. W. Harrington, ANAL. CHEM., **41**, 523 (1969).

(2) N. Margalit, Ph.D. thesis, Drexel University, Philadelphia, Pa., 1969.

(3) C. N. Reilley and D. T. Sawyer, "Experiments for Instrumental Methods," McGraw-Hill, New York, N.Y., 1961.

(4) L. C. Kenauses, E. C. Evers, and C. A. Kraus, *Proc. Nat. Acad. Sci. U.S.*, **49**, 141 (1963).